Faults and fractures in central West Greenland: onshore expression of continental break-up and sea-floor spreading in the Labrador – Baffin Bay Sea

Robert W. Wilson, Knud Erik S. Klint, Jeroen A.M. van Gool, Kenneth J.W. McCaffrey, Robert E. Holdsworth and James A. Chalmers

The complex Ungava fault zone lies in the Davis Strait and separates failed spreading centres in the Labrador Sea and Baffin Bay. This study focuses on coastal exposures east of the fault-bound Sisimiut basin, where the onshore expressions of these fault systems and the influence of pre-existing basement are examined. Regional lineament studies identify five main systems: N–S, NNE–SSW, ENE–WSW, ESE–WNW and NNW–SSE. Field studies reveal that strike-slip movements predominate, and are consistent with a ~NNE–SSW-oriented sinistral wrench system. Extensional faults trending N–S and ENE–WSW (basement-parallel), and compressional faults trending E–W, were also identified. The relative ages of these fault systems have been interpreted using cross-cutting relationships and by correlation with previously identified structures. A two-phase model for fault development fits the development of both the onshore fault systems observed in this study and regional tectonic structures offshore. The conclusions from this study show that the fault patterns and sense of movement on faults onshore reflect the stress fields that govern the opening of the Labrador Sea – Davis Strait – Baffin Bay seaway, and that the wrench couple on the Ungava transform system played a dominant role in the development of the onshore fault patterns.

Keywords: faults and fractures, extensional tectonics, wrench systems, sedimentary basins, basement reactivation, West Greenland

_____

R.W.W., K.J.W.M. & R.E.H., *Reactivation Research Group, Department of Earth Sciences, University of Durham, Durham DH1 3LE, UK.* E-mail: *robert.wilson@durham.ac.uk*
K.E.S.K., J.A.M.v.G. & J.A.C., *Geological Survey of Denmark and Greenland, Øster Voldgade 10, DK-1350 Copenhagen K, Denmark.*

Introduction

Pre-existing heterogeneities in the continental crust, such as shear zones and terrain boundaries, have long been known to influence the structure and development of later deformation events (Butler *et al.* 1997; Holdsworth *et al.* 1997, and references therein). The sedimentary basins of the Labrador Sea – Baffin Bay region are situated west of Greenland (Fig. 1) and are early Cenozoic failed spreading centres (Chalmers & Pulvertaft 2001), separated by the Davis Strait. The orientation of the Davis Strait relative to the proposed spreading centres in the Labrador Sea and Baffin Bay is consistent with the geometry of an 'extensional transform zone' (Taylor *et al.* 1994). Steep basement fabrics of the Nagssugtoqidian orogen trend highly obliquely to these offshore structures (Fig. 1) and coincide with this 'step-over zone' in the Davis Strait. Fault systems fundamental to the development of sedimentary basins in the Davis Strait are exposed onshore in West Greenland. In this project, the onshore fault systems of central West Greenland were studied in order to improve
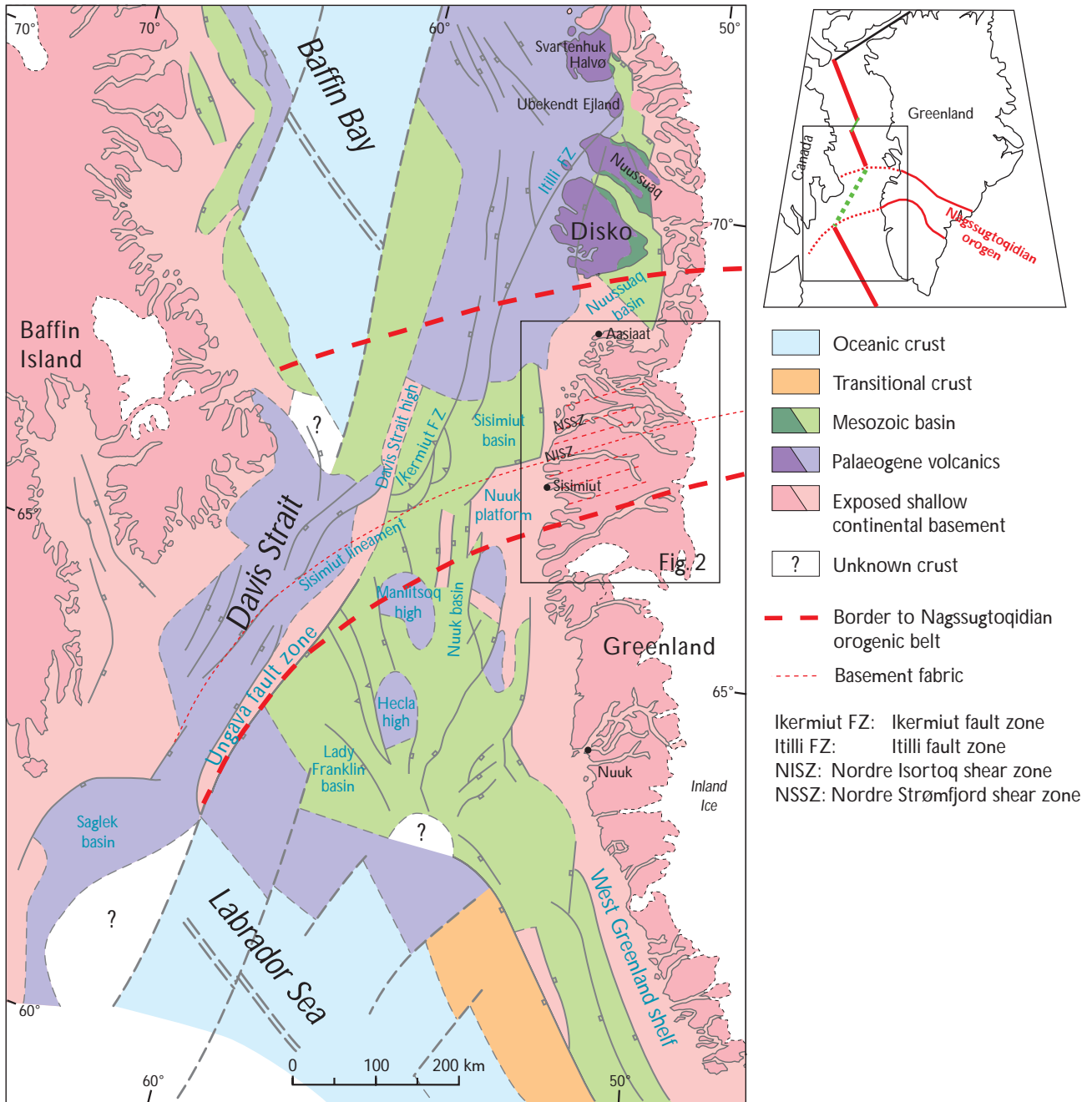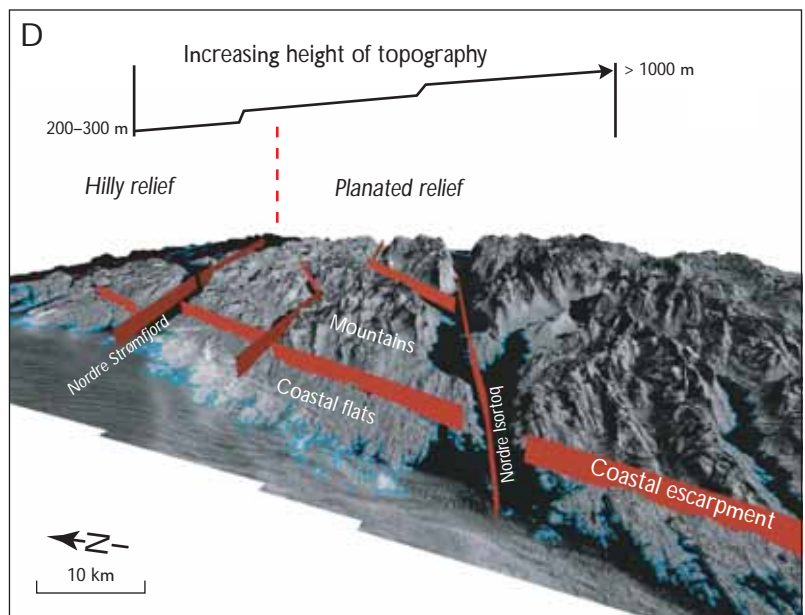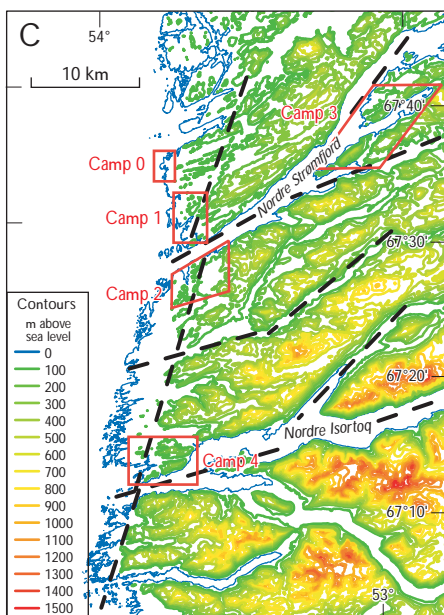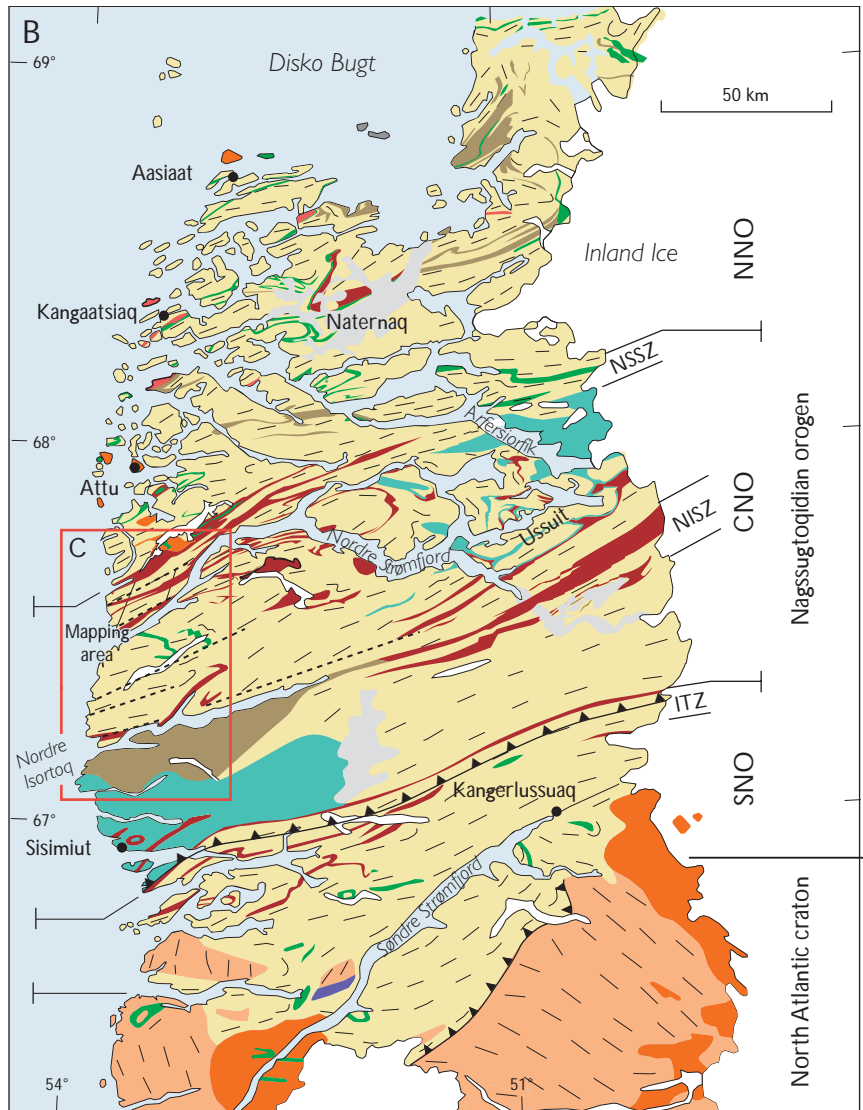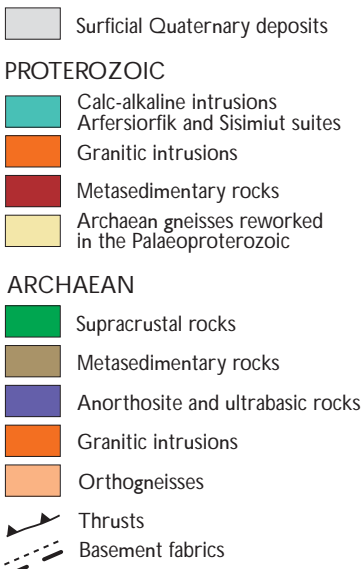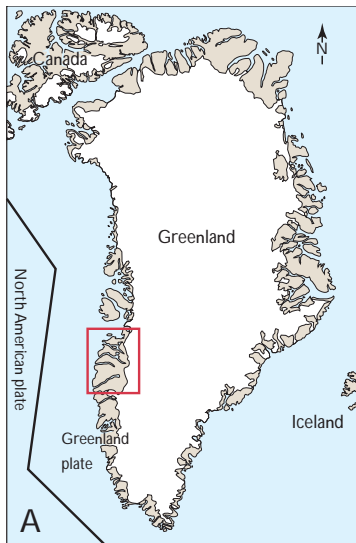
Fig. 1. Regional tectonic map of the offshore geology of the Labrador Sea – Baffin Bay area between Canada and Greenland. Modified from Chalmers & Pulvertaft (2001).

Facing page:

Fig. 2. Geological map of the Nagssugtoqidian orogen of central West Greenland (modified from Escher & Pulvertaft 1995). **A**: Outline map of Greenland highlighting the region covered in Fig. 2B. **B**: Geological map of the Nagssugtoqidian orogen showing main lithological units and basement structures. **C**: Topographic contour map of the central coastal area showing the field camps chosen for this study (camps 0 to 4); **black dashed lines** highlight major topographic escarpments. **D**: 3-D model view of NNE-trending coastal escarpment, constructed in ArcGIS by draping a Landsat image onto a topographic model. Abbreviations used: **SNO**, **CNO** and **NNO** are the southern, central and northern Nagssugtoqidian orogen, respectively. **ITZ**, Ikertôq thrust zone; **NISZ**, Nordre Isortoq shear zone; **NSSZ**, Nordre Strømfjord shear zone.

A

Canada

N

Greenland

North American plate

Greenland plate

Iceland

B

69°

Disko Bugt

Aasiaat

50 km

Inland Ice

NNO

Kangaatsiaq

Naternaq

Nagssugtoqidian orogen

NSSZ

Arfersiorfik

68°

CNO

NISZ

Attu

Ussuit

C

Nordre Strømfjord

Mapping area

ITZ

SNO

Nordre Isortoq

Kangerlussuaq

67°

Sisimiut

Sondre Strømfjord

North Atlantic craton

54°

51°

Legend

Surficial Quaternary deposits

PROTEROZOIC

Calc-alkaline intrusions Arfersiorfik and Sisimiut suites

Granitic intrusions

Metasedimentary rocks

Archaean gneisses reworked in the Palaeoproterozoic

ARCHAEAN

Supracrustal rocks

Metasedimentary rocks

Anorthosite and ultrabasic rocks

Granitic intrusions

Orthogneisses

Thrusts

Basement fabrics

C

54°

10 km

Camp 3   67°40'

Camp 0

Camp 1   Nordre Strømfjord

67°30'

Camp 2

67°20'

Nordre Isortoq

Camp 4

67°10'

53°

Contours
m above sea level

0
100
200
300
400
500
600
700
800
900
1000
1100
1200
1300
1400
1500

D

Increasing height of topography   > 1000 m

200–300 m

Hilly relief   Planated relief

Nordre Strømfjord

Mountains

Coastal flats

Nordre Isortoq

Coastal escarpment

N

10 km

the understanding of the role played by basement reactivation in offshore basin development.

In the summer of 2003 field work was carried out in an area along the coast stretching from Nordre Strømfjord (Nassuttooq) in the north, to Nordre Isortoq in the south (Figs 2, 3). This area was selected because it is believed that two ENE-striking Palaeoproterozoic shear zones, the Nordre Strømfjord shear zone and the Nordre Isortoq shear zone, were reactivated and played an important role in the development of the Mesozoic to Tertiary sedimentary basins. The western projection of the Nordre Isortoq shear zone appears to coincide with the southern faulted boundary of the Sisimiut basin offshore (Figs 1, 2). In addition, the offshore basins occur close to the coast in this area, and the offshore extensional faults that drop the top of the basement down to 3 km below sea level, within 10 km west of the coast, are believed to correlate with fault escarpments onshore in this area.

Tectonic and geological setting

Offshore

The Labrador Sea and Baffin Bay formed during divergent plate motion between Greenland and North America during the early Cenozoic (Chalmers & Pulvertaft 2001, and references therein). The extensional basins of Baffin Bay and the Labrador Sea are separated by a bathymetric high in the Davis Strait (Fig. 1). This transverse ridge is interpreted as a complex sinistral-shear transform fault zone, known as the Ungava fault system (Fig. 1; Chalmers *et al.* 1995). Extensional faulting and tectonic subsidence are thought to have commenced in the early Cretaceous, at the same time as sea-floor spreading in the North Atlantic south of the Charlie Gibbs fracture zone. Opening started during the Paleocene (Chian & Louden 1994; Chalmers & Laursen 1995), and sea-floor spreading appears to have ceased by the Oligocene.

Interpretation of seismic reflection data has revealed the existence of a number of sedimentary basins offshore western Greenland (Chalmers *et al.* 1995; Whittaker 1995). One such basin is the deep Sisimiut basin, located in the Davis Strait to the west of the Nordre Strømfjord region (Fig. 1). At about 10 km west of the coast, the top of the basement is at *c.* 3 km depth, while there is no cover preserved on top of basement exposed onshore. Therefore, the eastern border of the basin must be a major fault, but it is located too close to the coast to have been surveyed by a seismic experiment. The orientation of this bounding fault is likely to follow the NNE–SSW trend of
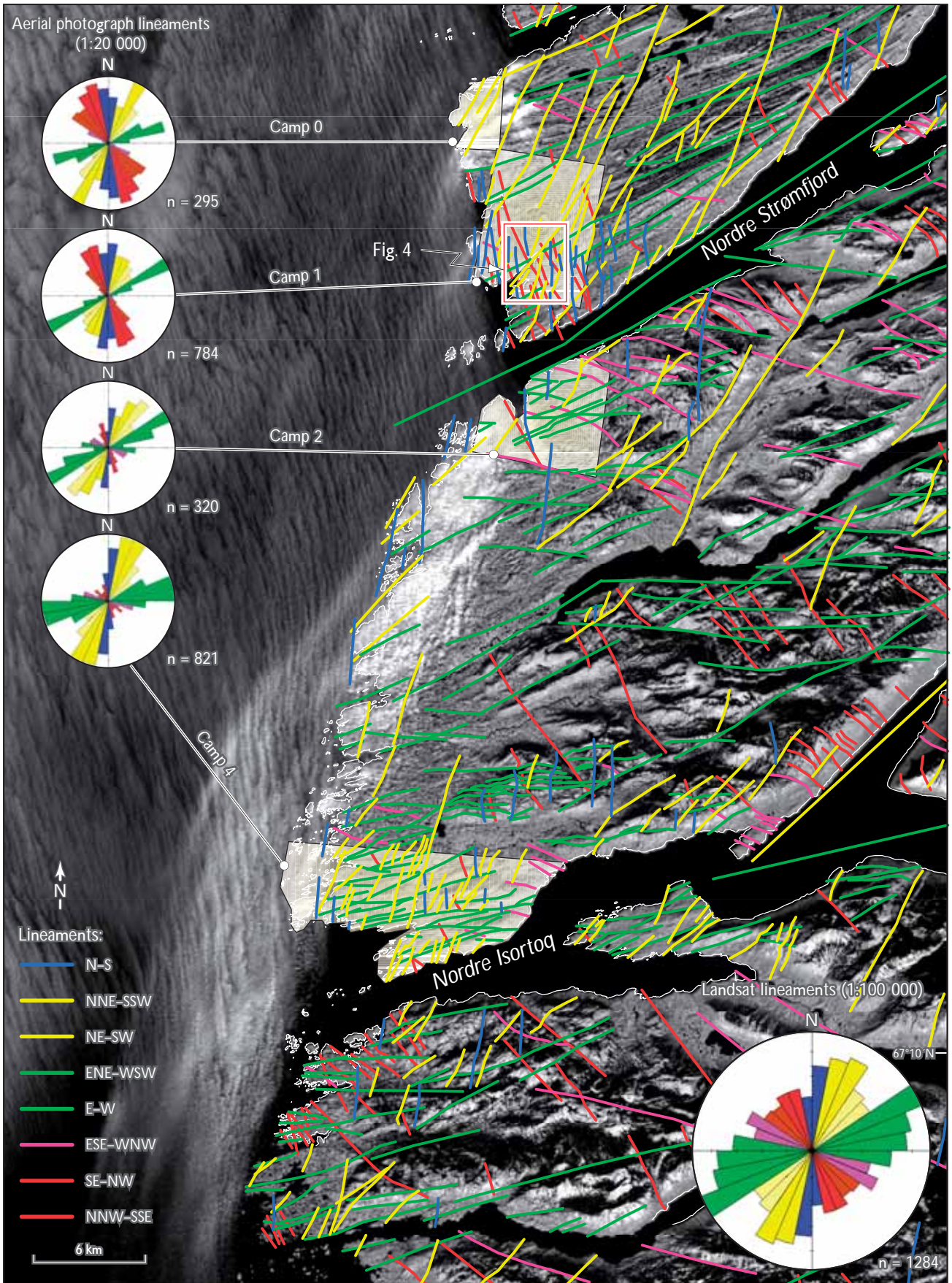
the coastline. The western margin of the Sisimiut basin is the NNE–SSW-trending Ikermiut fault zone (Fig. 1), a transpressional flower structure developed along the transform fault (Ungava fault zone) between the North American and Greenland plates (Fig. 2) formed during the Palaeogene (i.e. it cuts early Eocene strata; Chalmers & Pulvertaft 2001). The Nukik platform lies to the south of the Sisimiut basin and is separated from it by a line of ENE- and E-trending faults that coincide with the offshore extension of the Nordre Isortoq shear zone onshore (Figs 1, 2). It has therefore been proposed that the faults at the southern margin of the basin developed by reactivation of basement shear zone structures in the central Nagssugtoqidian orogen. These faults affect Mesozoic sediments and are overstepped by Paleocene sediments, so that the latest significant movement on them must have been prior to the end of the Paleocene.

Onshore

Onshore exposures in central West Greenland, from Søndre Strømfjord in the south to Disko Bugt in the north, comprise high-grade gneisses of the Palaeoproterozoic Nagssugtoqidian orogen (Fig. 2; Ramberg 1949; van Gool *et al.* 2002). The Nagssugtoqidian orogen is a 300 km wide belt of predominantly Archaean orthogneisses, Palaeoproterozoic paragneisses and intrusive rocks, that were reworked during Palaeoproterozoic orogenesis (van Gool *et al.* 2002). These basement rocks form ENE-trending linear belts of steeply dipping gneisses, some of which are crustal-scale shear zones (i.e. the Nordre Strømfjord and Nordre Isortoq shear zones, Fig. 2), which alternate with zones dominated by kilometre-scale fold structures (van Gool *et al.* 2002). The Nagssugtoqidian orogen is divided into three tectonic segments: the southern, central and northern Nagssugtoqidian orogen (Fig. 2; Marker *et al.* 1995). The onshore research in this study lies entirely within the granulite facies orthogneisses of the central Nagssugtoqidian orogen, which is bound to the north by the

Facing page:
Fig. 3. Lineament map of the main study area derived from lineament mapping of a Landsat TM image at 1:100 000 scale (total 1284 lineaments), using ArcGIS. The main rose diagram (bottom right) shows the distribution of lineaments for this map, while smaller rose diagrams (left) show results from aerial photograph analyses (at 1:20 000 scale) for each field camp. **Green**, system 1; **blue**, system 2; **red**, system 3; **yellow**, system 4; **purple**, system 5. **Red box** shows the position of Fig. 4.

Aerial photograph lineaments
(1:20 000)

N

n = 295

Camp 0

N

n = 784

Camp 1

Fig. 4

N

n = 320

Camp 2

N

n = 821

Camp 4

N

Lineaments:

— N–S
— NNE–SSW
— NE–SW
— ENE–WSW
— E–W
— ESE–WNW
— SE–NW
— NNW–SSE

6 km

Nordre Strømfjord

Nordre Isortoq

Landsat lineaments (1:100 000)

N

67°10′N

n = 1284

189

Nordre Strømfjord shear zone (Marker *et al.* 1995; van Gool *et al.* 2002) and to the south by the Ikertôq thrust zone (Fig. 2).

Indirect topographic evidence from geomorphological investigations has suggested that late (Mesozoic or Cenozoic) onshore fault movements may have occurred (Bonow 2004). For example, in some of the larger inlets and valleys, characteristic recent shelly marine sands can be observed up to 30 m above sea level. These are likely to have been uplifted due to isostatic rebound following glacial retreat. However, variations in elevation of these palaeoshorelines may also result from differential vertical fault movements or differential unloading. On the larger scale, the Nordre Strømfjord shear zone marks a major change between two landscape types (Japsen *et al.* 2002). South of the Nordre Strømfjord shear zone topography is planated, with flat mountain tops forming a plateau that gradually increases in height southwards from 500 to 1000 m (Fig. 2C, D). In contrast, north of the Nordre Strømfjord shear zone, the land has a hilly relief with a relatively flat and low-lying topography with isolated hills up to 300 m high. Locally, the change in landscape type occurs across a more than 500 m high, ENE–WSW-oriented escarpment that drops down to the north (Fig. 2).

There is also a pronounced NNE–SSW-oriented escarpment almost 1 km high that drops down to the west between Nordre Strømfjord and Nordre Isortoq (Fig. 2). This major escarpment separates low-lying (50–150 m high) coastal flats to the west from the much higher (500 m+) mountains to the east (Fig. 2) and can be traced for over 80 km, from Sisimiut in the south to Nordre Strømfjord in the north. Similar escarpments can be observed in the near offshore on both bathymetric and horizon maps of depth to basement, thus supporting the theory that onshore structures reflect those offshore.

Methods

The present study combines regional to outcrop-scale mapping and regional studies of remotely sensed data to determine fault-fracture geometries, distribution, relative timing and kinematics in selected key areas of central West Greenland.

Regional studies comprised satellite image and aerial photograph analysis at a variety of scales (1:500 000; 1:100 000; 1:20 000) in order to identify lineaments and other geological structures (e.g. variations in lithology, fabric intensity, faults, fractures).

Field investigations were carried out in the well-exposed Precambrian basement rocks in key areas of interest that were identified during aerial photograph analysis prior to departure. A number of field camps were used during the mapping (Fig. 2C). Camp 0 was located at Inussuk, a site visited previously in 2002 (Japsen *et al.* 2002). Camps 1 and 2 were located on the north and south shores of Nordre Strømfjord, while camp was on the north shore of Nordre Isortoq. Camp 3 was farther inland, and is not analysed further in this study.

During field work, fault and fracture systems were mapped, and the following structural data were collected for statistical/structural analysis:

- Fault attributes including: orientation; kinematics; fault surface characteristics; mineralisation.
- Relative age relationships.
- Structural/statistical analyses to determine kinematic patterns.

Over 200 pseudotachylite and mica-bearing fault-rock samples were also collected from different fault sets at various localities in order to date the fault movements using $^{40}Ar/^{39}Ar$ geochronology (results to be discussed elsewhere). All field data were geospatially located (to 5 m resolution) using Global Positioning System (GPS) waypoint collection, and were subsequently stored in a computer database with links to Geographic Information System (GIS) based maps.

Fault and fracture characterisation

Fractures include all brittle structures such as joints, fissures, cracks, veins, etc. that are not faults, bedding or cleavage surfaces, and are larger than the grain size of the rock. In general, fractures are defined as dominantly tensile (mode I) cracks, and as such, they are associated with characteristic stress, strain and displacement fields. They are distinguished from small faults by distinctive surface textures and lack of shear displacements. *Faults* are mapped where distinct offsets have been identified, often with a development of slip striae on the surface (slickenlines). Criteria for determining the sense of movement were based on methods outlined in McClay (1987) and Petit (1987).

In the present study faults were classified as:

- Normal (extensional dip / oblique-slip fault).
- Reverse (compressional dip / oblique-slip fault).
- Strike-slip faults (dextral or sinistral).

The classification of faults and fractures into systems was primarily based on the orientation of the structures (i.e.

Fig. 4. Age relationships interpreted from cross-cutting relationships of lineament systems derived from aerial photographs for camp 1. Four dominant lineament trends are apparent: N–S (system 2), NNE–SSW (system 4), ENE–WSW (system 1), and NNW–SSE (system 3). Through cross-cutting relationships a relative order of fault development is apparent, as indicated across the bottom of the image.
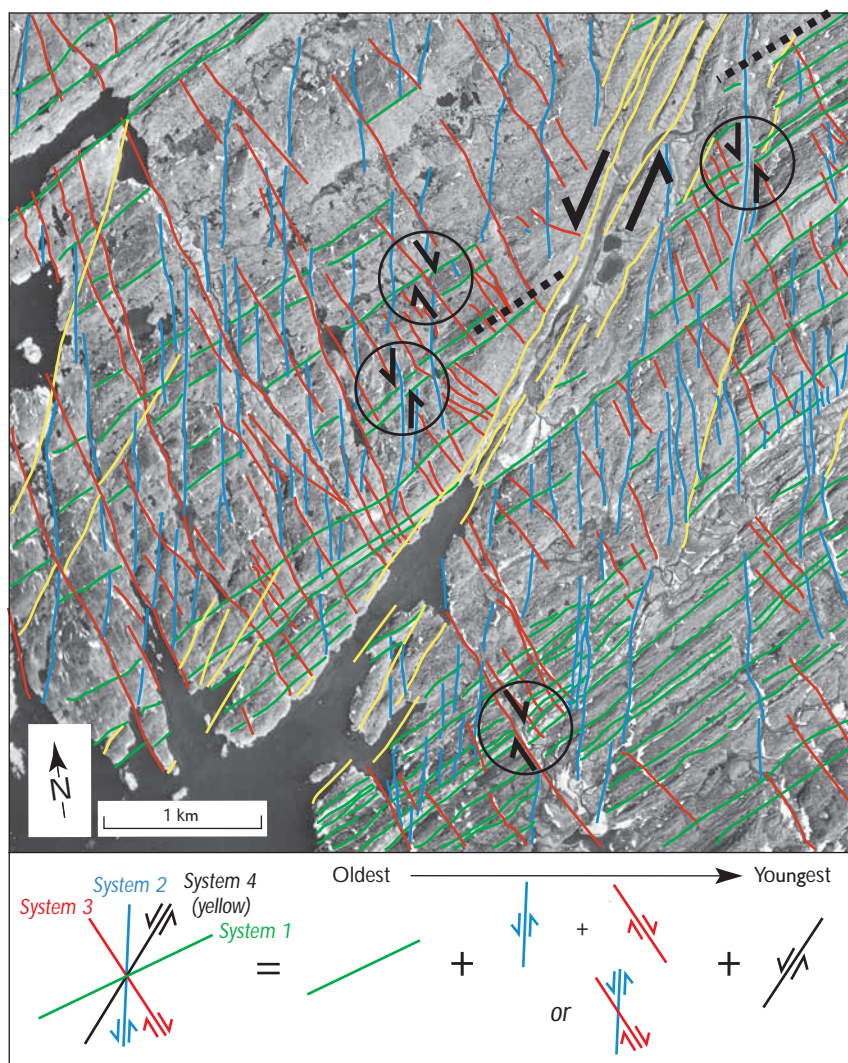
trend of lineament or strike of plane). Structures with different orientations can reflect different deformation phases, but in complex fault zones developed in three-dimensional (3-D) strain fields, multiple fault and fracture orientations may develop during a single event (see e.g. De Paola *et al.* 2005). Therefore further classification needs to be applied, either through systematic fracture properties (such as surface type or mineralisation), or through kinematic studies, in order to determine if only one or several phases of deformation are apparent.

Fault and fracture measurement technique

In order to accurately classify the fault and fracture systems, populations of at least 50 fractures/faults were measured at most localities. Faults were classified according to type (normal/reverse dip-slip faults or dextral/sinistral strike-slip faults). Fault orientations and the directions of slickenlines (when observed) were measured, and the following characteristics recorded:

- *Surface shape:* The overall fracture shape (metre-scale) was described as listric, planar, undulating or irregular.
- *Surface roughness character:* The surface roughness character (millimetre scale) was described as smooth, rough or slickenside (striae).
- *Other features:* Some fractures/faults have a filling of iron oxide precipitates, quartz crystals, epidote, or preferential growth of other crystals on the surface showing the slip direction. Special types of fractures such as conjugate shear fractures, en échelon fractures, plumose jointing etc. were noted if present.

Lineament mapping

Lineament maps for the central Nagssugtoqidian orogen (Fig. 3) were plotted from Landsat TM images and aerial photographs at a variety of scales (1:500 000 and 1:100 000 for Landsat images and 1:20 000 for aerial photographs). Images were georeferenced and displayed in a GIS environment and the lineaments picked by hand. After interpretation, lineaments were then refined using digital terrain model (DTM) analysis and compared to pre-existing geological maps of the region (e.g. Henriksen *et al.* 2000). As the data are stored in a GIS, attribute data for each lineament (i.e. trend; length; offset; other features) were also measured or calculated and stored. Spatial analysis and rose plotting tools in ArcView GIS were used to analyse the orientation (Fig. 3) and spatial distribution of these structures.

A more detailed analysis of selected areas was then carried out at 1:20 000 scale using aerial photographs. As image resolutions are much higher in aerial photographs (2 m pixel size), particular attention was paid to how the lineaments interact with topography (e.g. V-ing into valleys, etc.) to gain a better understanding of their overall geometry. Generally all lineaments picked appear to have a steep dip as only minor interactions with topography were observed. Attention was also paid to cross-cutting relationships between lineaments in an attempt to determine the relative timing of structures (Fig. 4).

Lineament systems

In total 1284 lineaments have been identified from Landsat TM images (pixel size 30 m) at 1:100 000 scale (Fig. 3). Lineaments derived from both Landsat and aerial photographs have been grouped into systems based on their orientation. Five main lineament systems (N–S, NNE–SSW, ENE–WSW, ESE–WNW, and NNW–SSE) have been identified (Fig. 3; Table 1).

System 1 structures (green; Figs 3, 4) are oriented ENE–WSW (~060–090° trend), and are pervasively distributed across the region. This system has a trend similar to the Nordre Strømfjord and Nordre Isortoq fjords, and lies parallel to the regional basement fabric (foliation, gneissic banding, and shear zones; van Gool *et al.* 2002). Note that as these lineaments may represent either faults or basement fabrics, care must be taken when analysing these quantitatively. In an attempt to minimise the amount of oversampling, only the most pronounced lineaments (e.g. most weathered out) that mark a distinct change in structure were mapped, while those that are clearly basement fabrics (i.e. those showing ductile features such as folds) were not.

System 2 lineaments (blue; Figs 3, 4) are N–S oriented (trend ~350–010°), and often show sinistral offsets of pre-existing structures (basement fabrics). This system can be traced from Nordre Isortoq to the northernmost part of the investigated area (Fig. 3), and previous investigations indicated that they may continue as far north as Aasiaat, Disko and Nuussuaq (Japsen *et al.* 2002). The fault zones are closely spaced (100–500 m), and strike-slip separations of up to 30 m have been observed.

System 3 lineaments (red; Figs 3, 4) are NNW–SSE oriented (trend ~140–170°). They are closely spaced (50–100 m), and offsets of marble beds show net dextral separations in the order of 20–40 m (Fig. 4). This system is most pronounced in the Nordre Strømfjord shear zone, and less dominant in the Nordre Isortoq shear zone (see rose diagrams in Fig. 3).

System 4 lineaments (yellow; Figs 3, 4) are oriented NNE–SSW (trend ~010–040°) and are strongly developed in the Nordre Strømfjord shear zone region (camps 0 and 1, Fig. 3). These structures show apparent sinistral strike-slip separations of up to 400 m in the westernmost part of the study area. The spacing between them increases from approximately 500 m at the coast, to approximately 2 km farther inland. The same lineament directions were encountered at camps 2 and 4, south of Nordre Strømfjord, where these structures are shorter and more discontinuous, possibly due to differences in rock type and fabric between the two areas.

System 5 lineaments (purple; Fig. 3) consist of E–W to ESE–WNW (trend ~090–120°) -oriented structures. The valleys that distinguish this system are generally 10–30 m wide and have a curved trend. This system appears to be mostly localised into two specific areas: the first of these lies in the fold belt south of Nordre Strømfjord (Fig. 3), and the second is located south of Sisimiut (Fig. 1).

Relative timings

Figure 4 shows an aerial photograph of an area around camp 1 where an apparent order of lineament development can be deduced. The oldest structures appear to be system 1 (green), and in this area these structures appear to be basement fabrics in the form of alternating layers of semipelite and marble up to 100 m thick (Henriksen *et al.* 2000). System 2 (blue) structures show sinistral offsets of these lithological layers, while system 3 structures (red) show dextral displacements. In Fig. 4, system 3 structures appear to dominantly cross-cut system 2 structures, but this is not always the case as in some areas the reverse is true (system 2 cross-cutting/displacing system 3). As there

Table 1. Main characteristics for each fault system, identified from remote sensing and outcrop studies

Lineament system	Orientation	Sense of movement	Comments
System 1	ENE–WSW	• Normal (dip-slip) • Reverse (dextral oblique-slip) • Dextral and sinistral strike-slip	• Basement-parallel to subparallel • Multiple phases of movement
System 2	N–S	• Sinistral strike-slip • Normal (dip-slip)	• Closely spaced (100–500 m) • Displacements range between 0.2 and 30 m for individual faults • May show an en échelon to irregular trend
System 3	NNW–SSE	• Dextral strike-slip • Normal (dip-slip and oblique-slip)	• Dominant fracture/joint trend is associated with this system • Closely spaced (50–100 m) • Marble layers show displacements in the order of 20–40 m
System 4	NNE–SSW	• Sinistral strike-slip	• Major subvertical faults and fault zones • Generally associated with wide (> 50 m) valleys • Exposed fault cores show complex fracture sets associated with strike-slip movements
System 5	E–W to ESE–WNW	• Dextral strike-slip	• Localised to the fold belt south of Nordre Strømfjord and north of the Nordre Isortoq shear zone • Prominent structures at regional scale (i.e. from Landsat and aerial photos) but not at outcrop • Spatially associated with compressional faults (i.e. system 1 reverse faults)

is evidence for systems 2 and 3 mutually cross-cutting each other, and also because apparent movements are compatible with a conjugate system of strike-slip faults, it is possible that they are contemporaneous. Cross-cutting all other systems are the NNE-trending system 4 lineaments, suggesting that they are likely to be the youngest structures, or at least have experienced the most recent movements.

Other areas show a similar pattern of events, although some system 1 structures show evidence for younger movements (reactivation?), especially in areas around camps 2 and 4. System 5 is not represented in Fig. 4 as it was not observed at camp 1. This system is marked by quite wide (30–50 m) valleys, thus making its displacements difficult to determine; however, as it is quite pronounced, it may be a more recent system.

Field observations

Four key areas were chosen for detailed fracture and fault analysis in the field (Fig. 3), based on their structural interest (i.e. their potential to enable all systems to be analysed) and accessibility. The first objective of the field work was identification of the lineaments picked from the aerial photographs. In most cases field observations proved that the lineaments correspond to major fault structures,

many of which are weathered out to leave gorges and river valleys (Fig. 5A–C). However, whilst many of the ENE–WSW-oriented system 1 structures are faults, others also correspond to basement fabric features, such as strongly foliated zones, lithological contacts and shear zones (Fig. 5D). Therefore care must be taken in any quantitative geometric or spatial analysis of this system.

After a regional reconnaissance from each field camp, detailed structural analysis was carried out. Ninety outcrop locations were investigated in the four camps, distributed along the coast between Nordre Isortoq and just north of Nordre Strømfjord (Fig. 2). In total c. 1700 faults and fractures were measured and described.

Fault geometries

A wide range of *fracture* orientations were observed (Fig. 6A), with dominantly N–S and NNW–SSE strikes and an overall mean fracture plane of 167/89E. Various *fault* orientations can be separated out in the field (dominant trends are N–S and ENE–WSW), showing a range of slip movements and shear senses (Fig. 6B–F). Dominant fault movements appear to be strike-slip (71% of faults recorded show strike-slip movements), although extensional and compressional faults were also apparent.
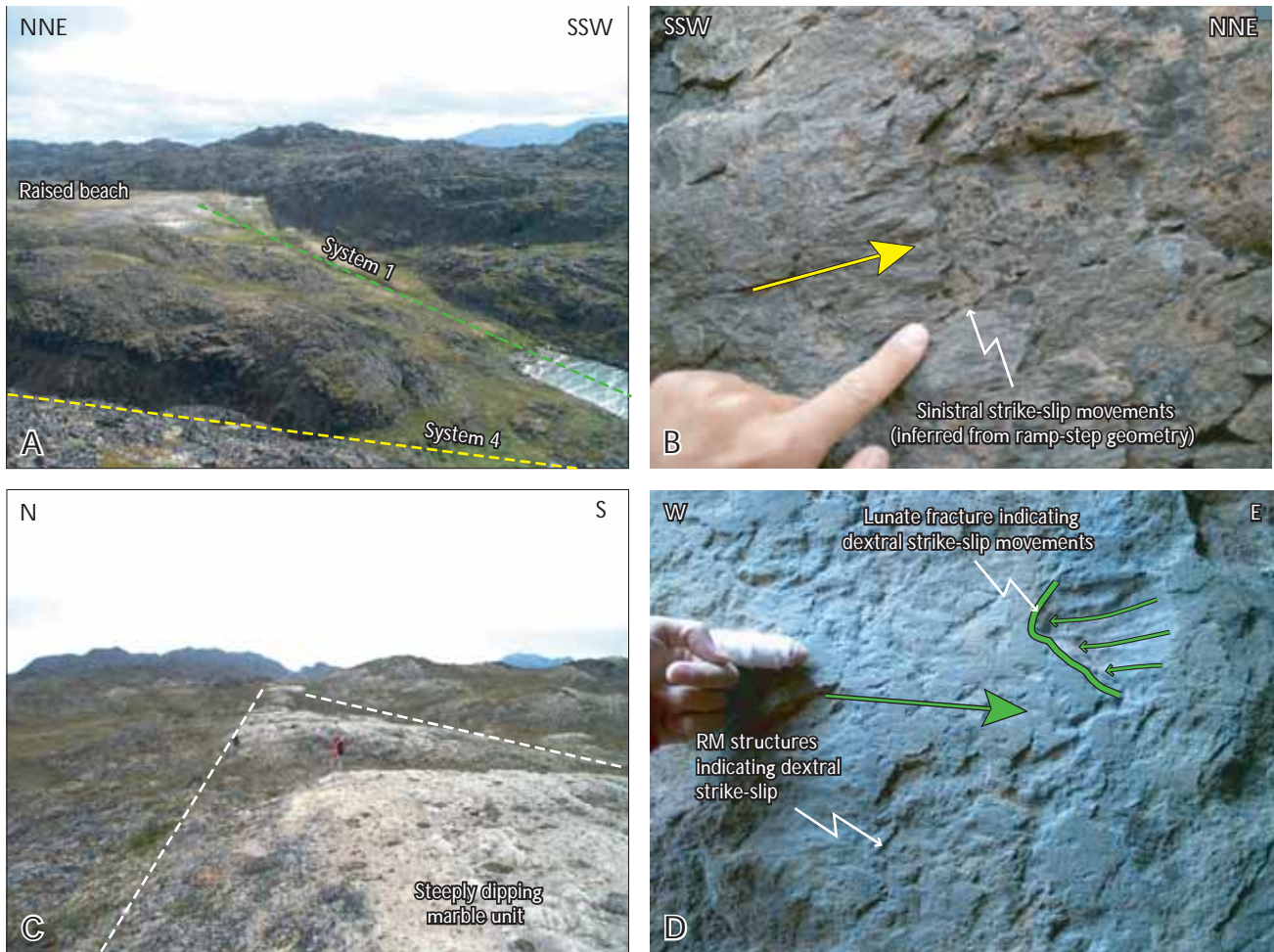
Fig. 5. Field identification of lineaments picked from Landsat and aerial photographs. **A**: Two major gorges/valleys trending ENE and NNE near camp 1; these correspond to major lineament systems 1 and 4, respectively. Fault core exposed within the NNE-trending stream bed (system 4) shows evidence for sinistral strike-slip faulting (Fig. 5B); fault movements on the ENE-trending basement-parallel valley (system 1) were not identified. **B**: Photograph of subhorizontal, sinistral strike-slip slickenlines observed within the fault core of the NNE-trending fault (system 4) identified in Fig. 5A. **C**: Some ENE-trending (system 1) lineaments correspond to basement fabrics such as steeply dipping (and tightly folded) marble units. **D**: Other basement parallel lineaments, however, do show evidence for brittle fault movement, as identified in this ENE-trending fault core (fault movement criteria defined by secondary fracture indicators, i.e. RM and lunate fractures, outlined in Petit 1987).

A set of ENE–WSW-oriented faults (green planes/mean poles in Fig. 6) appear to reactivate strong basement fabrics in the Nordre Strømfjord and Nordre Isortoq shear zones. These faults correspond to system 1 lineaments and exhibit various forms of fault movement (e.g. extensional, compressional and strike-slip; Fig. 6B–F). Faults corresponding to systems 2 (N–S, blue), 3 (NNW–SSE, red) and 4 (NNE–SSW, yellow) can also be easily distinguished from the fault data in Fig. 6. However, lineament system 5 (E–W to ESE–WNW, purple) is not apparent. As previously discussed this system appears to be a more geographically localised system (i.e. local to areas south of the Nordre Strømfjord and Nordre Isortoq shear zones), and correspond to zones dominated by reverse fault move-ments (Fig. 6B) and a small number of ESE-trending dextral strike-slip faults (Fig. 6E).

Fault systems corresponding to lineament systems 2, 3 and 4 appear to consist of parallel fault zones separated by non-faulted, but generally strongly fractured rock. The fault zones range typically between 1 and 50 m in width (Fig. 5B) and consist of multiple parallel faults with variable spacing. These zones are commonly located in pronounced valleys and gorges (Fig. 5A), so characterisation of fault planes was often difficult as the valley floors are generally covered by recent sediment and vegetation.
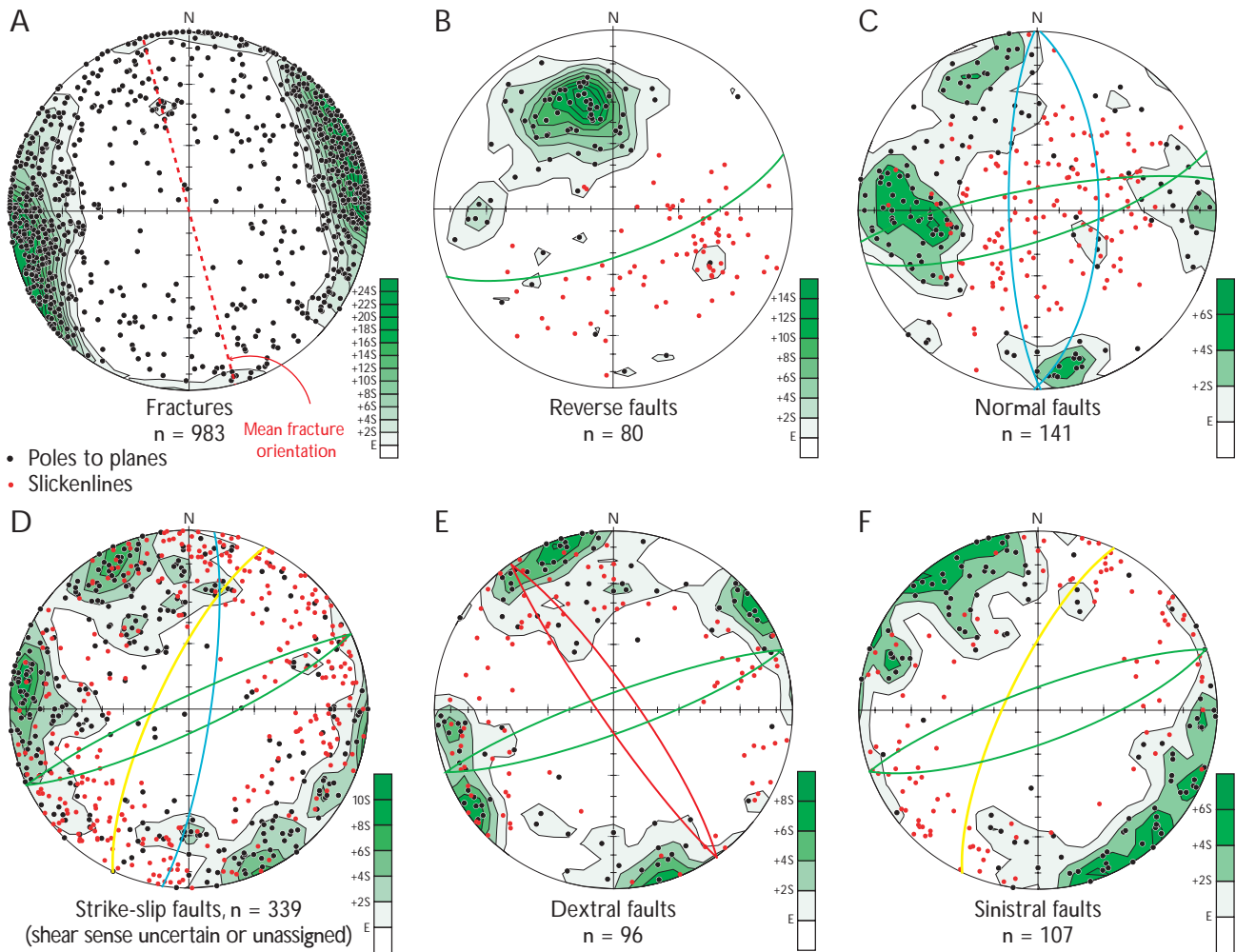
Fig. 6. Lower hemisphere, equal area stereographic projections of all fault and fracture data collected at camps 1, 2 and 4 (total number of measurements = 1746). A: Fractures (i.e. planes showing no evidence for slip). B: Reverse faults. C: Normal faults. D: Strike-slip faults with undetermined sense of movement. E: Dextral strike-slip faults. F: Sinistral strike-slip faults. Black dots, poles to planes of fault and fracture surfaces. Red dots, slickenlines. Mean fault planes are also shown, coloured according to lineament/fault systems identified in Fig. 3. Poles to fault and fracture surfaces are contoured using a Gaussian weighting function; **n**, number of measurements for each plot. In the labels, **E** corresponds to the background value (calculated as number of points/100), while **S** = standard deviations above this value.

Fault kinematics

In addition to the characterisation of the faults and fractures in terms of their trend and distribution, they can also be described according to their movement patterns (see Table 1). The nature and timing of tectonic events that are responsible for the formation of these fault-fracture systems is quite complex. Multiple directions of slickenlines on several fault surfaces indicate that many faults were either reactivated or that individual faults exhibit curved movement trajectories consistent with complex strain histories.

Strike-slip faulting

Strike-slip slickenlines account for 71% of those observed and were observed on all main fault geometries or systems. Multiple orientations of strike-slip faulting are common in wrench-dominated fault systems due to the development of Riedel, P and X shears (e.g. Woodcock & Schubert 1994).

Basement parallel faults (system 1, green) show both dextral and sinistral movements (note, RM structures – Petit 1987 – associated with R-shears suggest dextral movements on basement faults in Fig. 5D). NNW-trending (system 3, red) faults appear to correspond to dextral movements. N-trending faults (system 2, blue) appear to
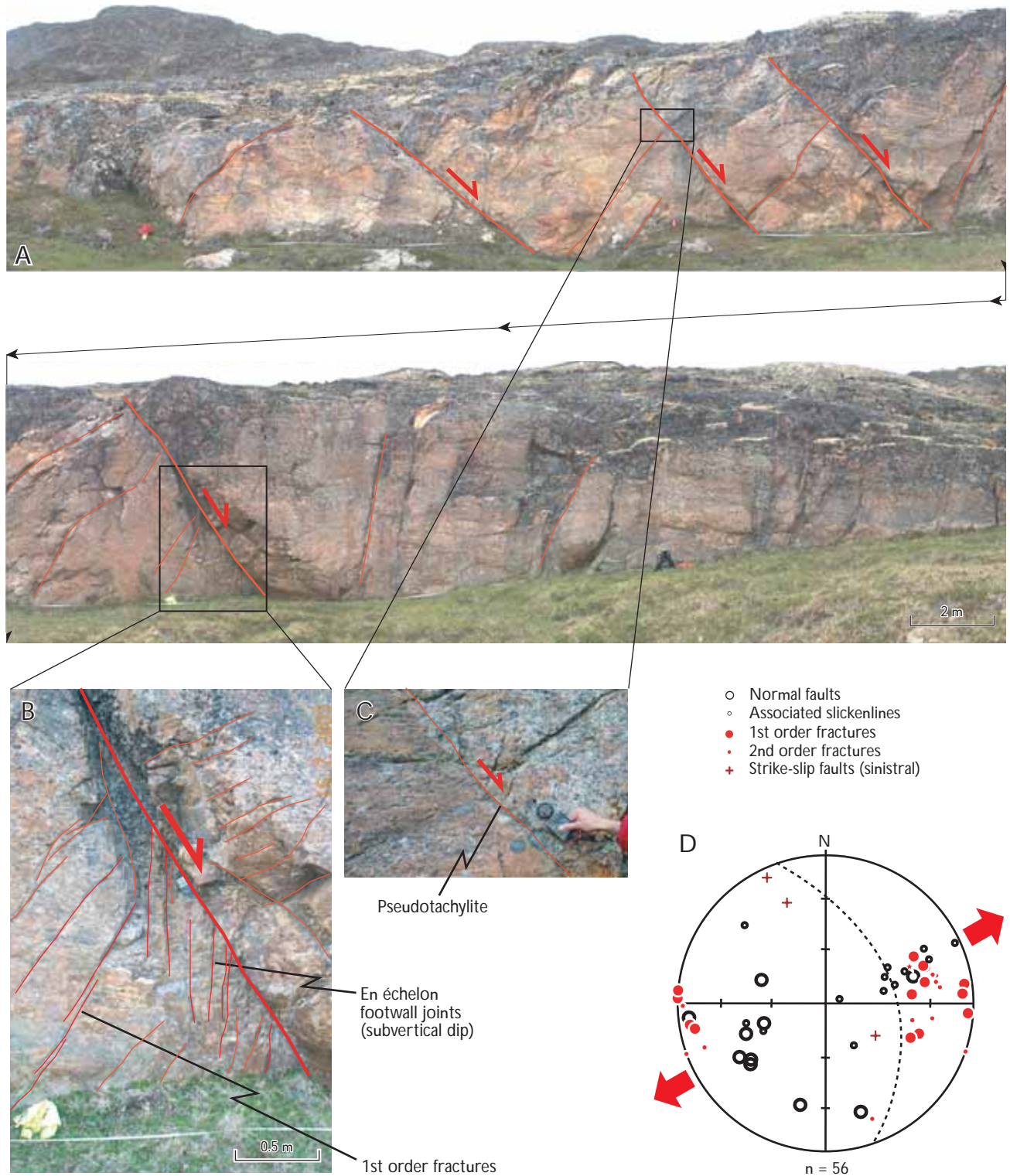
Fig. 7. **A**: Panoramic photograph showing exposures of a series of parallel ENE-dipping extensional faults, in the vicinity of camp 1. **B** and **C**: close-up photographs showing en échelon fracturing on the footwall of normal faults and pseudotachylite fault exposure in more detail. **D**: Lower hemisphere, equal area stereographic projection of poles to planes, and associated slickenlines, for faults and fractures observed at the outcrop of Fig. 7A. Fault orientations and kinematics suggest ENE–WSW extension as indicated by stress arrows (**red**); **n**, number of measurements.
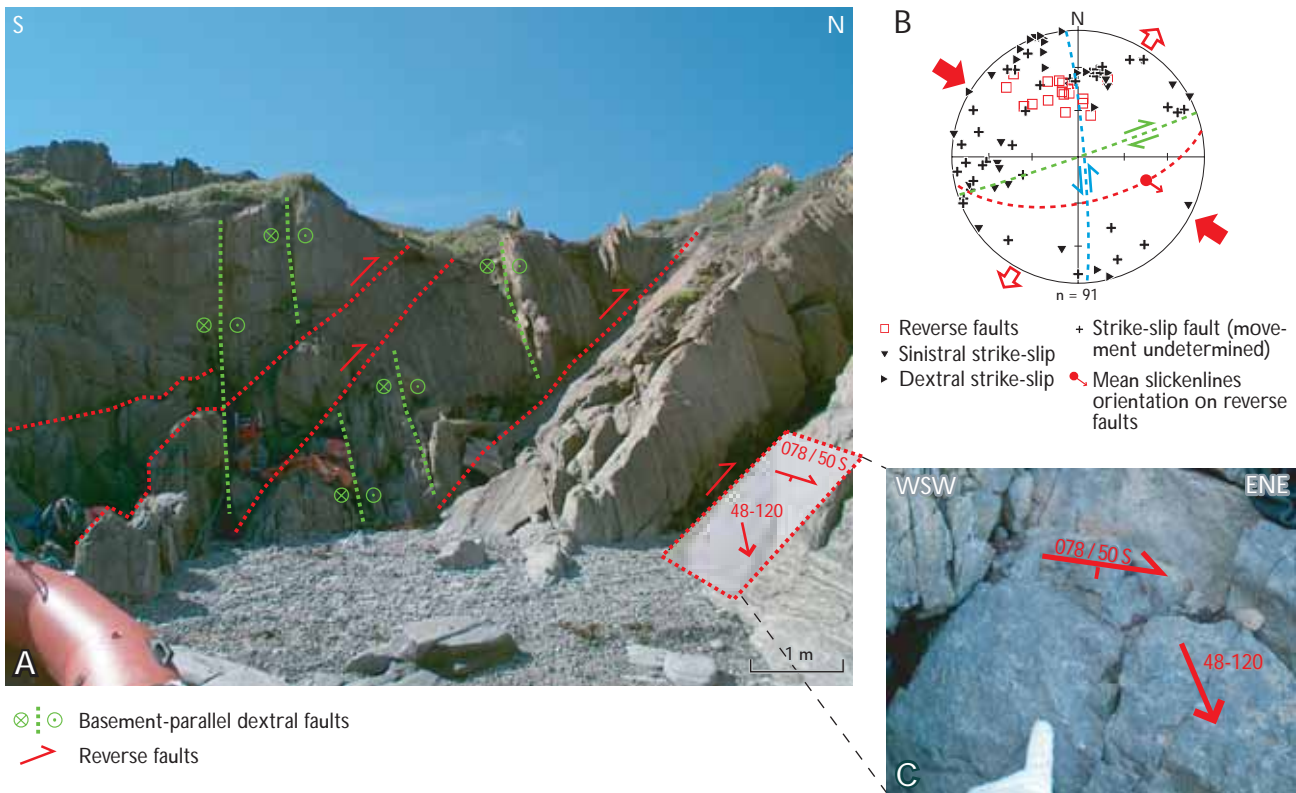
Fig. 8. **A**: Exposure of a localised set of reverse faults near camp 4. **B**: Lower hemisphere, equal area stereographic projections of poles to structures observed at the locality of Fig. 8A. Three dominant fault sets are apparent: basement parallel – i.e. ENE-trending – reverse and dextral strike-slip faults, and a set of sinistral faults oriented N–S (e.g. along the large rock face in shadow). Slickenline orientations and relative fault movements suggest ESE–WNW compression as indicated by stress arrows (**red**); **n**, number of measurements. **C**: Photograph of surface of reverse fault, showing dextral-oblique slickenlines (mean slickenline orientation 45/120, see stereonet). Note that faults coloured in **red** here highlight thrust faults and do not refer to system 3 faults as in other figures.

show both dextral and sinistral movements, while NNE-trending faults (system 4, yellow) are sinistral structures (Fig. 6D–F).

Extensional faulting

Although all five fault systems show dominantly strike-slip movements, normal and oblique-slip components of displacement were also recorded on some sets. These faults appear to have two dominant orientations, N–S (system 2) and ENE–WSW (system 1; Fig. 6C). In some areas NNW–SSE (system 3) -oriented structures also appear to be normal faults (Fig. 7), but these are not the dominant orientations in bulk analyses (Fig. 6). Field observations suggest that strike-slip movements post-date dip-slip.

Compressional faulting

Reverse faults (Figs 6B, 8) appear to be confined to areas close to camps 2 and 4, and to be spatially associated with system 5 lineaments. These faults strike parallel or sub-parallel to basement structures (ENE–WSW to E–W, Fig. 6B) and exhibit dextral-oblique slickenlines, which plunge towards the ESE (Figs 6B, 8).

As these compressional or thrust faults are only found on the southern shore of Nordre Strømfjord and the northern shore of Nordre Isortoq (i.e. abutting against major basement shear zones) it is possible that these structures are the result of local transpressional thrust faulting, which may be linked to steps in the en échelon sinistral fault system (system 4). Field observations suggest these compressional faults post-date most other fault and fractures. However, at camp 4, a N–S sinistral strike-slip fault appears to cross-cut these thrusts (Fig. 8B).

Fractures and joints

A diverse array of fracture orientations was recorded. Dominant orientations vary from NW–SE through to NNE–SSW. The orientation of the mean plane is NNW–SSE. All fractures recorded showed no evidence for shear movement (i.e. rough surfaces and with no apparent offsets) and are thus interpreted as opening mode 1 fractures and suggesting extension directions varied from *c.* E–W to NE–SW.

Interpretation and discussion

An overall summary of each of the fault systems identified through remote sensing (i.e. lineament mapping) and field studies is presented in Table 1. In this section we discuss the possible interpretations and implications of these observations.

Fault development

System 1 (ENE–WSW) faults and fractures appear to be the oldest structures, however multiple slip vectors and apparent fault movements suggest that there has been activity on this system during later tectonic episodes (note that system 1 faults are apparent in all stereoplots for all fault types, Fig. 6B–F). These lie parallel to the pre-existing Nagssugtoqidian basement fabric, which dates at *c.* 1.8 Ga (van Gool *et al.* 2002).

Cross-cutting relationships interpreted from analysis of aerial photographs suggest that the next systems to develop were systems 2 and 3 (Fig. 5). It is difficult to determine if one of these systems predates the other as mutually cross-cutting relationships can be seen; however, it does appear that system 3 is the more pervasive system and thus may be more recent.

Strike-slip movements and offsets on systems 2 (N–S) and 3 (NNW–SSE) suggest that, if active at the same time, these would represent a strike-slip conjugate system. In such cases the inferred extension vector would trend ENE–WSW, subparallel to system 1 foliation-parallel faults. This extension vector is also consistent with the dip-slip fault movements seen locally on these same fault systems.

These strike-slip movements appear to be preceded by dip-slip extensional movements. System 2 (N–S) is the dominant extensional fault orientation in the area (Fig. 6C), while some localities showed small populations where NNW–SSE-oriented extensional faults represent the preferred trend (e.g. Fig. 7). These faults are indicative of E–W to ENE–WSW extension. This extension cannot, however, explain the apparent basement-parallel (system 1) extensional faults, which suggest an apparent NNW–SSE extension. These ENE-trending normal faults have also been observed in seismic interpretations and are thus important structures regionally.

These two extensional fault sets show a quadrimodal fault distribution, i.e. four sets of fault planes (Fig. 6C). If regarded as two separate fault sets, this geometry would suggest two separate extension directions (E–W and NNW–SSE); however an alternative to this is that these faults formed contemporaneously under three-dimensional strain (Reches 1983; Nieto-Samaniego & Alaniz-Alvarez 1997). As one set of normal faults trends parallel to a pre-existing plane of weakness (e.g. basement fabric) it is likely that basement reactivation played a role in the development of these faults, and that this has lead to formation of extensional faults oblique to the regional extension. The regional tectonic setting would fit with 3-D strain as the area borders the transfer zone between two extensional basins, i.e. is a transtensional deformation zone (Dewey 2002; De Paola *et al.* 2005).

Geoffroy *et al.* (1998) recorded similar fault geometries and kinematics farther north in Disko and Nuussuaq (Fig. 1). Their interpretation is that strike-slip and dip-slip faulting developed during a single tectonic episode of WSW–ENE extension, which is in agreement with a model of 3-D transtensional strain.

As the stereoplots in Fig. 6 show, strike-slip faults are the dominant fault type in the area (as mentioned above, 71% of all faults measures are strike-slip) and these appear to post-date extensional movements. All fault systems show evidence for strike-slip movements. System 1 (ENE–WSW) exhibits both dextral and sinistral senses of shear, systems 3 (NNW–SSE) and 5 (ESE–WNW) show dextral shear, while systems 2 (N–S) and 4 (NNE–SSW) are dominated by sinistral shear movements. System 4 faults (NNE–SSW) appear to cross-cut all other fault sets, and are characterised by major fault zones (Fig. 5). These major sinistral strike-slip structures lie subparallel to the sinistral Ikermiut and Ungava fault zones that dominate the Davis Strait offshore (Fig. 1). Assuming a ~NNE-trending sinistral wrench system for the study area, strike-slip fault movements on each system appear to correlate closely with synthetic (R) and antithetic (R') Reidel shears, and also with synthetic P and antithetic X shears typical of a plane strain wrench tectonic regime (Fig. 9; Woodcock & Schubert 1994).

Compressional faults appear to be relatively late structures (although cross-cut by ~N–S-trending sinistral faults) and are localised in areas of strong basement fabric (i.e.

Fig. 9. **A**: Diagram showing fault systems and their corresponding movements. **B**: Strain ellipse for a NNE–SSW (~010–190°) -oriented sinistral wrench system, showing Riedel (**R** and **R'**), **P** and **X** shears (Woodcock & Schubert 1994). Also shown are the regional stress vectors ($\sigma 1$ and $\sigma 3$). Systems 2 (sinistral) and 5 (dextral) correspond to R' and R shears, while systems 1 (dextral) and 4 (sinistral) correspond to P and X shears. System 3 corresponds to normal fault sets in Fig. 9B; however, dominant movements on this system were dextral.

NNE–SSW (10–15°) wrench system: 55–60° extension, 145–150° compression
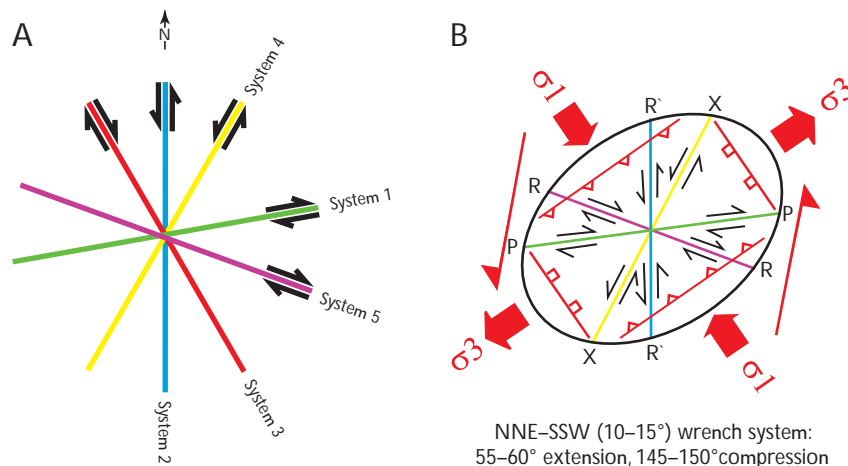
shear zones). These faults strike parallel to basement fabrics and indicate an oblique compression (from the ESE or SE; Fig. 8). Offshore there is evidence for thrusting in a similar orientation along the Ikermiut fault zone (Fig. 1). Positive flower structures have been identified (Chalmers & Pulvertaft 2001) and are interpreted as inversion structures formed at a restraining bend during sinistral strike-slip along the Ungava transform fault, during the early Eocene (*c.* 54–49 Ma, Chalmers & Pulvertaft 2001). If trends of basement shear zones (outlined in Fig. 2) are continued alongstrike offshore they appear to coincide with these transpression zones within the Ikermiut fault zone. It is possible that thrusts observed onshore have formed in a similar way to those offshore with basement shear zones acting as restraining bend structures, thus leading to localised compressional zones. Furthermore, slickenlines on the reverse faults suggest a compression from the ESE or SE (Figs 6B, 8), which is consistent with the compressional axis for a sinistral wrench system (i.e. NE–SW extension and NW–SE compression; Fig. 9).

Regional comparison and implications

A key prerequisite for building tectono-stratigraphic models is being able to date each tectonic event. As all onshore exposures in this part of West Greenland are in Precambrian basement rocks, there are no stratigraphic markers for constraining the timing of Phanerozoic tectonic events. Relative timing has been inferred from various cross-cutting relationships in the field and from lineament analysis, but is open to different interpretations. In the absence of age data that constrain the absolute age(s) of fault activity, comparisons with offshore models and with data collected in other onshore areas are used here to infer ages for events in our tectonic model (see Table 2 for a summary).

Regional onshore correlations

Farther north in the region of Disko and Nuussuaq, onshore faulting episodes can be dated relative to the deposition of basaltic lavas and the sedimentary systems during Campanian to Eocene times (Geoffroy *et al.* 1998; Storey *et al.* 1998; Chalmers *et al.* 1999; Dam *et al.* 2000). Dam & Sønderholm (1998), Dam *et al.* (2000) and Dam (2002) document at least three phases of faulting recorded in the sedimentary record prior to Paleocene volcanism. Cretaceous–Paleocene sediments on Nuussuaq show distinct unconformities, with incised valleys and submarine canyons, reflecting disturbances in early Campanian, Maastrichtian and early Paleocene times. These unconformities and channels are thought to have formed in response to structural movements associated with regional NE–SW rifting (and also the arrival of the North Atlantic plume in the latter two cases).

[40]Ar/[39]Ar dating has revealed that volcanism commenced in West Greenland between 60.9 and 61.3 Ma and that 80% of the Paleocene lava pile was erupted in less than 1 Ma (Storey *et al.* 1998). These lavas show a distinct coastal flexure (Geoffroy *et al.* 1998, 2001; Larsen & Pulvertaft 2000), presently expressed by seaward dipping basalt lavas. This flexure has an arcuate course, striking NW–SE in southern Svartenhuk Halvø and northern Ubekendt Ejland, turning through N–S in south-west Ubekendt Ejland to NE–SW in north-west Nuussuaq and finally to N–S in north-west Disko (Fig. 1; Geoffroy *et al.* 1998, 2001; Larsen & Pulvertaft 2000). Numerous dykes cut these lavas (e.g. see figs 4 and 5 in Larsen & Pulvertaft 2000), and so do various fault sets (Geoffroy *et al.* 1998). The timing of the various phases of volcanic eruption, dyke emplacement, and block faulting relative to one another is still a matter of debate. Geoffroy *et al.* (1998) presented detailed structural evidence suggesting that fault and dyke intrusion on Disko took place during tilting of lava sys-

Event #	Timing and event	Offshore tectonic structures	Onshore tectonic structures
5 (Youngest)	Pliocene to Pleistocene tilting	• Subsidence	• Uplift? • Possible reactivation of systems 1–4 as normal faults
4	Eocene Labrador sea-floor spreading (Ungava system)	• N- to NNE-trending sinistral transverse fault system (Ungava fault zone). • Local transpressional and transtensional faulting (e.g. Ikermiut fault zone)	• Faults consistent with NNE-oriented sinistral wrench system: NNE-trending (system 4) faults and basement-parallel (system 1) faults active as antithetic X and synthetic P shears • Systems 2 (reactivation) and 5 active as Reidel shears • Local transpressional thrust faulting observed near camps 2 and 4, associated with steep basement fabrics
3	Late Cretaceous to early Paleocene extension	• N-trending faults in Davis Strait (E–W extension) leading to formation of the Sisimiut Basin offshore	• Systems 1, 2 (and 3?) faults all active as extensional faults during NE–SW to ENE–WSW extension (3D strain)?
2	Early or middle to late Cretaceous extension and thermal subsidence	• NW-trending normal faults in the Labrador Sea (SW–NE extension) • WSW–ENE faults bordering the Sisimiut basin to the south were active offshore during events 2 and/or 3	• Uncertain?
1 (Oldest)	Proterozoic and later localised reactivation	• Uncertain?	• Possible system 1 ENE–WSW foliation-parallel faulting prior to late Mesozoic?

tems. Geoffroy *et al.* (2001) then stated that NW–SE-oriented, flexure-parallel dykes in southern Svartenhuk yield dates of around 54.6 ± 0.6 Ma. This suggests that most of the coastal flexure is of Eocene age (or later?). Further evidence for this comes from north-west Nuussuaq where tilted lavas (Larsen & Pulvertaft 2000) have been dated at ~53 Ma (Storey *et al.* 1998).

Systems 2 (N–S) and 3 (NNW–SSE) extensional faults in this study appear comparable to faults that cross-cut these Paleocene basalt lavas (Geoffroy *et al.* 1998). Taking the dates outlined above for dyke emplacement which is believed to be associated with faulting, it would appear that our system 2 and 3 faults were active during Eocene times. Taking all these onshore tectonic timings into account it would then appear that the faults observed may have been active from late Cretaceous (Maastrichtian) through to Eocene times (Dam & Sønderholm 1998; Geoffroy *et al.* 1998, 2001; Chalmers *et al.* 1999; Dam *et al.* 2000; Larsen & Pulvertaft 2000; Dam 2002).

Normal fault orientations similar to systems 2 (N–S) and 3 (NNW–SSE) occur in and around the Nuussuaq basin (Fig. 1; Geoffroy *et al.* 1998; Chalmers *et al.* 1999) and are consistent with either ENE–WSW (Geoffroy *et al.* 1998) or E–W (Chalmers *et al.* 1999) extension. Chalmers *et al.* (1999) proposed that the N–S faults formed by E–W-oriented crustal extension, while associated ESE–WNW faults formed as a consequence of reactivation of shear zones in the underlying basement. Normal faults are dominantly N–S onshore (Fig. 6C), fitting with this model proposed by Chalmers *et al.* (1999). However, this implies that while Baffin Bay in the north and Labrador Sea in the south were undergoing ENE–WSW extension (deduced from dominant fault trends and earliest magnetic anomaly trends, Chalmers & Pulvertaft 2001), southern West Greenland and the Nuussuaq basin were undergoing E–W extension. A better explanation is that the Davis Strait at this time (i.e. prior to the onset of sea-floor spreading) lay in a transfer/step-over zone between two extensional basins, and that it was strongly influenced by basement fabrics such that this region experienced complex 3-D strain associated with regional ENE–WSW extension (Fig. 10). Onshore normal fault sets form a quadrimodal fault distribution (four sets of fault planes, Fig. 6C) consistent with 3-D strain.

This faulting is then subsequently dissected by N–S (system 2) and NNE–SSW (system 4) -oriented faults during the Eocene (Chalmers *et al.* 1999). The Itilli fault zone (Fig. 1) is one such NNE–SSW-oriented structure cutting through north-west Nuussuaq. This fault zone appears to be a left-lateral splay from the northern extension of the Ungava fault zone in the Davis Strait (Chalmers *et al.* 1999).

STAGE 1:
Late Cretaceous–Paleocene extension (NE–SW to ENE–SSW). Pre-existing basement anisotropy (Nagssugtoqidian orogenic belt) appears to influence fault patterns in the Davis Strait. Possible strain partitioning between basement-parallel and N–S-trending normal faults.
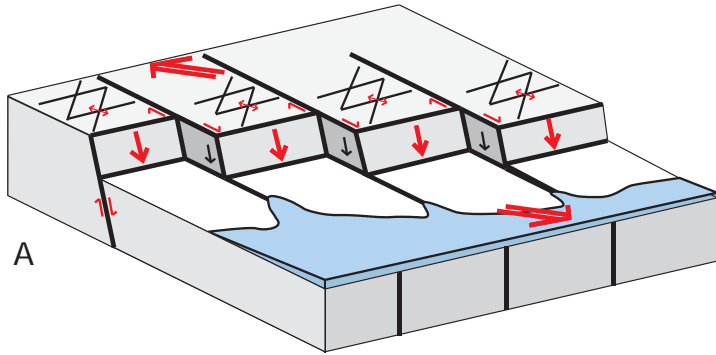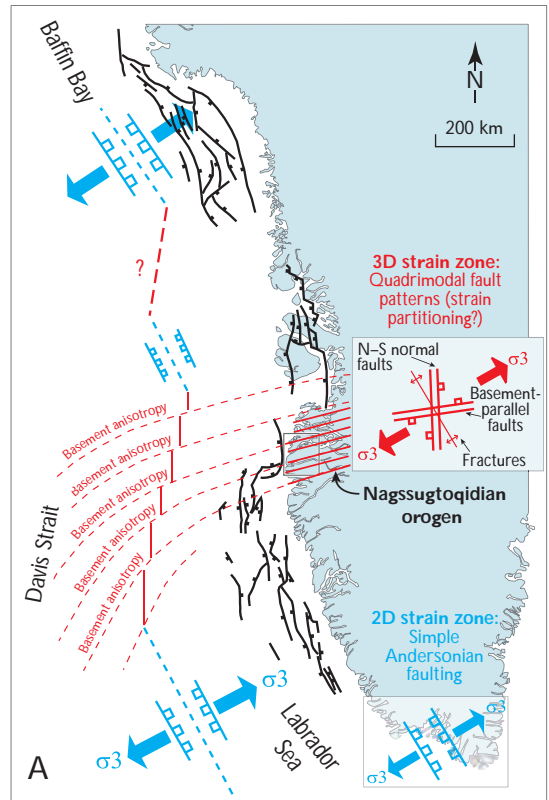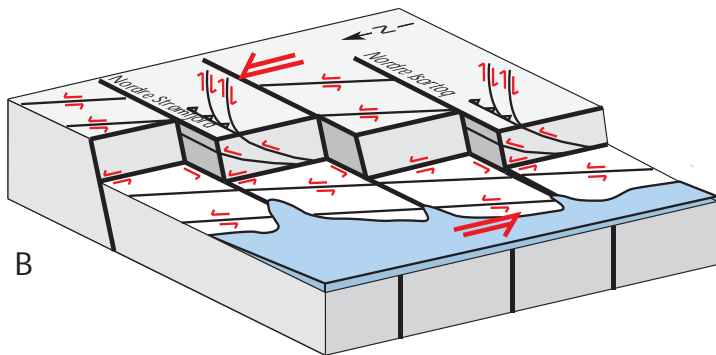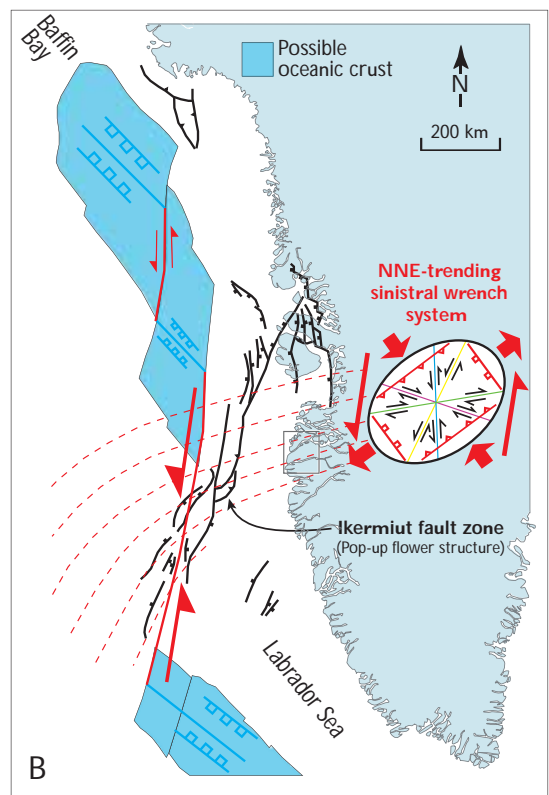
STAGE 2:
NNE-trending Eocene sinistral wrench system (NE to ENE extension, SE to SSE compression) reactivating earlier extensional faults and basement-parallel structures (e.g. thrust faults at camp 4, and the Ikermiut fault zone).

Fig. 10. Proposed two-stage tectonic model for the tectonic evolution of upper Mesozoic – Cenozoic extension within the Nagssugtoqidian orogen. Stage 1(**A**): N- and ENE-trending normal faults and dextral basement reactivation due to ENE–WSW extension. Stage 2 (**B**): N- and NNE-trending sinistral strike-slip faulting, and associated strike-slip wrench tectonic systems, with compressional structures (reverse faults) forming in zones of basement anisotropy (e.g. shear zones). **Block diagrams** show schematic cartoons outlining fault patterns observed onshore, while **maps** show the regional context, based on correlations between onshore and offshore fault structures.

201

Correlation with fault structures offshore

Fault patterns offshore in the Davis Strait exhibit similar *c*. N–S and ENE–WSW dominant orientations. The south and east bounding faults to the Sisimiut basin strike ENE–WSW and N–S respectively (Fig. 1). Significantly, the southern margin of the Sisimiut basin is coincident both in orientation and location with a major basement shear zone (the Nordre Isortoq shear zone), and is likely to have exerted a similar structural control to that interpreted for onshore. Block faulting has been dated via drilling as having taken place between the late Campanian and late Paleocene (Christiansen *et al.* 2001; Dalhoff *et al.* 2003), indicating that these extensional faults are of similar age to those associated with valley incision on Nuussuaq and north Disko (Dam & Sønderholm 1998; Dam *et al.* 2000; Dam 2002).

The Ungava fault zone with its associated fault systems (e.g. the Ikermiut fault zone) is the most prominent structure in the Davis Strait (Chalmers & Pulvertaft 2001). This NNE–SSW-oriented structure is interpreted as a transform fault zone showing sinistral shear, and has been linked to the Itilli fault zone (Fig. 1; Chalmers *et al.* 1999). System 4 (NNE–SSW) faulting onshore, around Nordre Strømfjord, is consistent with late sinistral strike-slip movements, and it is reasonable to suggest that this system is of similar age. As already discussed, offshore evidence for sinistral strike-slip movements can be seen in the Ikermiut fault zone on the western margin of the Sisimiut basin (Chalmers & Pulvertaft 2001) where transpressional thrusts (similar to compressional flower structures modelled in Dooley *et al.* 1999) appear to have formed in the restraining bend of a strike-slip fault (see fig. 6 of Chalmers & Pulvertaft 2001). These thrusts cut early Eocene mudstones, but are overlain by late Eocene sediments, providing further evidence for timing of these movements. This sinistral shear is thus a consequence of left-lateral movement of the Canadian plate relative to the Greenland plate along the Ungava transform system during sea-floor spreading in the Labrador Sea (Fig. 1).

Evidence for neotectonic faulting?

Chalmers (2000) presented evidence for Neogene uplift in offshore areas of central West Greenland, while recent onshore topographic and apatite fission-track data analysis has identified similar Neogene activity (Japsen *et al.* 2002, 2005). A common observation in this field area is the presence of raised beaches and palaeoshorelines, up to elevations 30 m above present sea levels (Fig. 5A). They are probably the result of isostatic readjustment following the removal of Pleistocene ice load. Topographically, the region appears to be divided into blocks, split by ENE-trending fjords and NNE-trending escarpments (Fig. 2C). These must be quite recent features as they have not been eroded during glacial activity (and may in fact be a consequence of it). The trend of system 4 faults (and also locally those of system 2) is generally parallel to the pronounced NNE-trending escarpment from Nordre Isortoq to Nordre Strømfjord onshore, and also to a similarly trending scarp near offshore (identified in bathymetry maps), and it is possible that these faults have been reactivated as normal faults during a recent tectonic event. This conjecture still needs to be verified, as the main escarpments were not studied in detail during our field work.

Summary

The observed fault and fracture systems reflect a brittle tectonic history that is ultimately related to far-field plate movements, uplift and basin formation. The development of Mesozoic to Cenozoic basins offshore West Greenland appears to be strongly controlled by faults. Therefore, knowledge of the fracture systems in the exposed Precambrian basement provides a valuable insight into fault geometries and kinematics during the development of offshore basins and potential hydrocarbon reservoirs. It also provides insights into the possible influence of basement reactivation.

Several possible tectonic-event models may be constructed for this region given the lack of definite ages for structures. Table 2 shows a basic summary of the relative timings of fault systems identified in this study relative to regional offshore tectonic models, while Fig. 10 presents a model for fault development based on the observations and correlations made in this study. The absolute timing of the fault activity onshore, as deduced from correlation to other fault systems with known ages, needs to be tested by dating of fault rock samples. A simple two-stage model has been outlined to explain the complex fault patterns exhibited in onshore exposures of the central Nagssugtoqidian orogen (Fig. 10).

The brittle tectonic evolution of the region appears to be dominated by NE–SW extension, which is consistent with the opening of the Labrador Sea and Baffin Bay. Only slight variations in the regional stress field are required to account for the diversity of fault orientations. According to Chalmers & Pulvertaft (2001) there was a 15° counter

clockwise rotation in spreading direction between the Paleocene and the Eocene in the Labrador Sea as opening started between Greenland and Europe, which is consistent with the two-stage model outlined in Fig. 10. In the early stages of opening, faulting was dominated by extensional structures (under 3-D strain conditions), favouring an E–W to ENE–WSW extension (Fig. 10A); however, as the Ungava transform fault developed, faulting became more wrench dominated (2-D plane strain), and suggests NE–SW extension (Fig. 10B). Variations in fault geometry reflect these changes in the regional stress field. However, the influence of basement structure also appears to have played an important role throughout (e.g. extensional faults not normal to the extension direction, and the apparent localised compressional zones associated with intense basement fabrics). Although most faults observed onshore trend highly obliquely to basement fabrics, fault patterns do appear to vary in areas of intense pre-existing structure (such as the Nordre Strømfjord and Nordre Isortoq shear zones) which suggest that the fabrics within the Nagssugtoqidian orogen may have had some influence on the fault complexity of the Davis Strait.

The conclusions from this study show that the fault patterns and sense of movement on faults onshore reflect the stress fields that govern the opening of the Labrador Sea – Davis Strait – Baffin Bay seaway, and that the wrench couple on the Ungava transform system played a dominant role in the development of the onshore fault patterns.

Acknowledgements

References

Bonow, J.M. 2004: Palaeosurfaces and palaeovalleys on North Atlantic previously glaciated passive margins – reference forms for conclusions on uplift and erosion. Ph.D. thesis. Thesis in Geography with Emphasis on Physical Geography **30**, 17 pp. + 4 articles. Stockholm University, Sweden.

Butler, R.W.H., Holdsworth, R.E. & Lloyd, G.E. 1997: The role of basement reactivation in continental deformation. Journal of the Geological Society (London) **154**, 69–71.

Chalmers, J.A. 2000: Offshore evidence for Neogene uplift in central West Greenland. Global and Planetary Change **24**, 311–318.

Chalmers, J.A. & Laursen, K.H. 1995: Labrador Sea: the extent of continental crust and the timing of the start of sea floor spreading. Marine and Petroleum Geology **12**, 205–217.

Chalmers, J.A. & Pulvertaft, T.C.R. 2001: Development of the continental margins of the Labrador Sea: a review. In: Wilson, R.C.L. *et al.* (eds): Non-volcanic rifting of continental margins: a comparison of evidence from land and sea. Geological Society Special Publication (London) **187**, 77–105.

Chalmers, J.A., Dahl-Jensen, T., Bate, K.J. & Whittaker, R.C. 1995: Geology and petroleum prospectivity of the region offshore southern West Greenland. Rapport Grønlands Geologiske Undersøgelse **165**, 13–21.

Chalmers, J.A., Pulvertaft, T.C.R., Marcussen, C. & Pedersen, A.K. 1999: New insight into the structure of the Nuussuaq basin, central West Greenland. Marine and Petroleum Geology **16**, 197–224.

Chian, D. & Louden, K.E. 1994: The continent-ocean crustal transition across the southwest Greenland margin. Journal of Geophysical Research **99**, 9117–9135.

Christiansen, F.G., Bojesen-Koefoed, J.A. & Chalmers, J.A. 2001: Petroleum geological activities in West Greenland in 2000. Geology of Greenland Survey Bulletin **189**, 24–33.

Dalhoff, F., Chalmers, J.A., Gregersen, U., Nøhr-Hansen, H., Rasmussen, J.A. & Sheldon, E. 2003: Mapping and facies analysis of Paleocene – Mid-Eocene seismic sequences, offshore southern West Greenland. Marine and Petroleum Geology **20**, 935–986.

Dam, G. 2002: Sedimentology of magmatically and structurally controlled outburst valleys along rifted volcanic margins: examples from the Nuussuaq basin, West Greenland. Sedimentology **49**, 505–532.

Dam, G. & Sønderholm, M. 1998: Sedimentological evolution of a fault-controlled early Paleocene incised-valley system, Nuussuaq Basin, West Greenland. In: Shanley, K.W. & McCabe, P.J. (eds): Relative role of eustasy, climate, and tectonism in continental rocks. Society of Economic Paleontologists and Mineralogists Special Publication **59**, 109–121.

Dam, G., Nøhr-Hansen, H., Pedersen, G.K. & Sønderholm, M. 2000: Sedimentary and structural evidence of a new early Campanian rift phase in the Nuussuaq Basin, West Greenland. Cretaceous Research **21**, 127–154.

De Paola, N., Holdsworth, R.E., McCaffrey, K.J.W. & Barchi, M.R. 2005: Partitioned transtension: an alternative to basin inversion models. Journal of Structural Geology **27**, 607–625.

Dewey, J.F. 2002: Transtension in arcs and orogens. International Geology Review **44**, 402–439.

Dooley, T., McClay, K. & Bonora, M. 1999: 4D evolution of segmented strike-slip fault systems: applications to NW Europe. In: Fleet, A.J. & Boldy, S.A.R. (eds): Petroleum geology of Northwest Europe, Proceedings of the 5th Conference, 215–225. London: Geological Society.

Escher, J.C. & Pulvertaft, T.C.R. 1995: Geological map of Greenland, 1:2 500 000. Copenhagen: Geological Survey of Greenland.

Geoffroy, J., Gélard, J.P., Lepvrier, C. & Olivier, P. 1998: The coastal flexure of Disko (West Greenland), onshore expression of the 'oblique reflectors'. Journal of the Geological Society (London) **155**, 463–473.

Geoffroy, J. *et al.* 2001: Southeast Baffin volcanic margin and the North American – Greenland plate separation. Tectonics **20**, 566–584.

Henriksen, N., Higgins, A.K., Kalsbeek, F. & Pulvertaft, T.C.R. 2000: Greenland from Archaean to Quaternary. Descriptive text to the geological map of Greenland, 1:2 500 000. Geology of Greenland Survey Bulletin **185**, 93 pp.

Holdsworth, R.E., Butler, C.A. & Roberts, A.M. 1997: The recognition of reactivation during continental deformation. Journal of the Geological Society (London) **154**, 73–78.

Japsen, P., Bonow, J., Klint, K.E.S. & Jensen, F.K. 2002: Neogene uplift, erosion and resedimentation in West Greenland. Field report summer 2002. Danmarks og Grønlands Geologiske Undersøgelse Rapport **2002/71**, 114 pp.

Japsen, P., Green, P.F. & Chalmers, J.A. 2005: Separation of Palaeogene and Neogene uplift on Nuussuaq, West Greenland. Journal of the Geological Society (London) **162**, 299–314.

Larsen, J.G. & Pulvertaft, T.C.R. 2000: The structure of the Cretaceous–Palaeogene sedimentary-volcanic area of Svartenhuk Halvø, central West Greenland. Geology of Greenland Survey Bulletin **188**, 40 pp.

Marker, M., Mengel, F., van Gool, J. and field party 1995: Evolution of the Palaeoproterozoic Nagssugtoqidian orogen: DLC investigations in West Greenland. Rapport Grønlands Geologiske Undersøgelse **165**, 100–105.

McClay, K.R. 1987: The mapping of geological structures (Geological Society of London handbook), 161 pp. London: John Wiley and Sons.

Nieto-Samaniego, A.F. & Alaniz-Alvarez, S.A. 1997: Origin and tectonic interpretation of multiple fault patterns. Tectonophysics **279**, 197–206.

Petit, J.-P. 1987: Criteria for the sense of movement on fault surfaces in brittle rocks. Journal of Structural Geology **9**, 597–608.

Ramberg, H. 1949: On the petrogenesis of the gneiss complexes between Sukkertoppen and Christianshaab, West Greenland. Meddelelser fra Dansk Geologisk Forening **11**, 312–327.

Reches, Z. 1983: Faulting of rocks in three-dimensional strain fields. II. Theoretical analysis. Tectonophysics **95**, 133–156.

Storey, M., Duncan, R.A., Pedersen, A.K., Larsen, L.M. & Larsen, H.C. 1998: $^{40}Ar/^{39}Ar$ geochronology of the West Greenland Tertiary volcanic province. Earth and Planetary Science Letters **160**, 569–586.

Taylor, B., Crook, K. & Sinton, J. 1994: Extensional transform zones and oblique spreading centres. Journal of Geophysical Research **99**(B10), 19707–19718.

van Gool, J.A.M., Connelly, J.N., Marker, M. & Mengel, F.C. 2002: The Nagssugtoqidian orogen of West Greenland: tectonic evolution and regional correlations from a West Greenland perspective. Canadian Journal of Earth Sciences **39**, 665–686.

Whittaker, R.C. 1995: A preliminary assessment of the structure, basin development and petroleum potential offshore central West Greenland. Open File Series Grønlands Geologiske Undersøgelse **95/9**, 33 pp., 6 maps.

Woodcock, N.H. & Schubert, C. 1994: Continental strike-slip tectonics. In: Hancock, P.L. (ed.): Continental deformation, 251–263. Oxford: Pergamon Press.